Geosci. Model Dev. Discuss., 3, 2051–2070, 2010
www.geosci-model-dev-discuss.net/3/2051/2010/
doi:10.5194/gmdd-3-2051-2010

Geoscientific Model Development Discussions

Simulation of atmospheric carbon dioxide variability with a global coupled Eulerian-Lagrangian transport model

Y. Koyama[1], **S. Maksyutov**[1], **H. Mukai**[1], **K. Thoning**[2], **and P. Tans**[2]

[1]National Institute for Environmental Studies, Tsukuba, Japan
[2]NOAA Earth System Research Laboratory, Boulder, USA

Received: 30 September 2010 – Accepted: 19 October 2010 – Published: 4 November 2010

Correspondence to: Y. Koyama (koyama.yuji@nies.go.jp)

Published by Copernicus Publications on behalf of the European Geosciences Union.

Abstract

This study assesses the advantages of using a coupled atmospheric-tracer transport model, comprising a global Eulerian model and a global Lagrangian particle dispersion model, for reproducibility of tracer gas variation affected by near field around observation sites. The ability to resolve variability in atmospheric composition on an hourly time scale and a spatial scale of several kilometers would be beneficial for analyzing data from continuous ground-based monitoring and upcoming space-based observations. The coupled model yields increased horizontal resolution of transport and fluxes, and has been tested in regional-scale studies of atmospheric chemistry. By applying the Lagrangian component to the global domain, we extend this approach to the global scale, thereby enabling global inverse modeling and data assimilation. To validate the coupled model, we compare model-simulated CO_2 concentrations with continuous observations at two sites operated by the National Oceanic and Atmospheric Administration, USA and one site operated by National Institute for Environmental Studies, Japan. As the purpose of this study is limited to demonstration of the new modeling approach, we select a small subset of 3 sites to highlight use of the model in various geographical areas. To explore the capability of the coupled model in simulating synoptic-scale meteorological phenomena, we calculate the correlation coefficients and variance ratios between deseasonalized model-simulated and observed CO_2 concentrations. Compared with the Eulerian model alone, the coupled model yields improved agreement between modeled and observed CO_2 concentrations.

1 Introduction

Here, we report the development and validation of a coupled atmospheric tracer transport model that comprises a global Eulerian grid model combined with a Lagrangian particle dispersion model. In principle, Lagrangian particle dispersion models (LPDMs) such as FLEXPART (Stohl et al., 1998) and STILT (Lin et al., 2003) can simulate highly resolved observation footprints and allow flexible choices regarding the resolution of

GMDD
3, 2051–2070, 2010

a simulation of the footprint, because they calculate the trajectory of each particle individually. LPDMs differ from Eulerian models in that they overcome a problem of a numerical diffusion. For example, in contrast to Eulerian models, a particle in an LPDM is not mixed with background air in a simulation grid; consequently, LPDMs avoid transport errors caused by numerical diffusion and the non-monotonic behaviour that is inevitable in higher-order schemes (Godunov, 1959).

Thompson (1971) developed an early model of particle diffusion that provided the foundation for subsequent LPDMs. Although LPDMs have been under development for a few decades, they have only recently become popular as a tool for investigating the transport processes associated with atmospheric events. This slow adoption of LPDMs has occurred because such models require abundant computer resources: to accurately describe a multi-day transport episode requires simulations of the separate trajectories of a large number of particles over multiple days. Since the 1990s, however, many studies have employed LPDMs (e.g., Zannetti, 1992; Uliasz, 1994; Rodean, 1996; Wilson and Sawford, 1996).

More recently, LPDMs have been used for various research applications at a regional scale (Lin et al., 2003, 2006, 2007; Paris et al., 2010; Warneke et al., 2009). When applying an LPDM for global analysis, a long-term integration is required (see Stohl et al., 2010); however, such an approach is less computationally efficient than the use of Eulerian models. This problem may be overcome by using a coupled model, in which the resolution of the flux data for an LPDM can be chosen independently from the resolutions of the simulation grid for a Eulerian model and its flux data. Several studies have investigated coupling between Lagrangian and Eulerian models at a regional scale (Vermeulen et al., 2006; Trusilova et al., 2010). The benefits of coupled transport modeling at regional and global scales can be fully realized by using emission inventories at 10 km resolution (Olivier et al., 2008; Gurney et al., 2009) or 1 km resolution (Kannari et al., 2007; Oda and Maksyutov, 2010). Hence, a coupled model can perform forward calculations with high-spatial-resolution surface fluxes, requiring less computation time than conventional Eulerian models. In the present study, we expand

GMDD
3, 2051–2070, 2010

the application of the coupled model to the global scale by using a global LPDM and a Eulerian model coupled at a time boundary rather than at a domain boundary, which is used in regional modeling. Thus, the spatial locations of coupling are not limited to a certain regional domain.

To develop the coupled model, we employ NIES transport model (NIES TM) (Maksyutov et al., 2008) as a Eulerian model and use FLEXPART version 3.2 as an LPDM. To validate the coupled model, we compare the modeled CO_2 concentrations with NOAA's continuous measurements at Barrow, USA (BRW; 71.32° N, 156.61° W) and Samoa (SMO; 14.25° S, 170.56° E) (Thoning et al., 2007). In this study, we used only the data which are passed through 3 quality control flags adopted by NOAA/ESRL (Earth System Research Laboratory). We also compare the modeled CO_2 concentrations with continuous observations obtained by NIES (National Institute for Environmental Studies) at Hateruma station (HAT; 24.05° N, 123.80° E) on the eastern end of Hateruma Island (Mukai et al., 2001), which is a small island (area, 12.5 km^2) located at the southwestern end of the Japanese Archipelago, 220 km east of Taiwan. The wind at this site is mainly from the southeast in summer and from the northwest in winter. Consequently, wintertime pollution events are common because of the transport of emissions from the Asian continent.

The main purpose of coupling an LPDM with a Eulerian model is to address the situation in which tracer variations are dominated by the surface flux around the station of interest. In this scenario, the reproducibility of short term synoptic-scale variability is more important than contributions from large-scale latitudinal gradients provided by a Eulerian model. In the Northern Hemisphere in particular, variations in CO_2 concentration are strongly affected by large-scale variability; that is, seasonal variations mainly induced by the respiration and photosynthesis of vegetation. Hence, the subtracting the seasonal variation is useful to assess the ability of the coupled model.

We extracted synoptic-scale variability from both simulated and observed CO_2 concentrations by subtracting the running average. We then calculated the correlation coefficients and the variance ratios between simulated and observed data.

GMDD
3, 2051–2070, 2010

2 Materials and methods

In the coupled tracer transport algorithm employed in this study, CO_2 transport is divided into two time periods: during the first stage, CO_2 concentrations are simulated by the Eulerian model globally at a medium resolution; during the second stage, the LPDM is used to simulate transport with corresponding fluxes at a higher resolution. The optimal duration of the second stage – the period of backward plume transport – is determined empirically as 7 days by comparing (1) the results of simulations with various Lagrangian transport periods and (2) observations at Hateruma. The results of a study by Gloor et al. (2001) indicate that a shorter period can be sufficient for other sites.

The simulated concentration at an observation site is predicted in four steps, as follows. (1) FLEXPART simulates 7-day back-plume transport, which represents the time-reversed trajectory of 10 000 air particles released from the location of interest. The actual transport time varies between 6.875 and 7 days, depending on the time of particle release, because coupling with the global Eulerian model occurs at a 3-hourly interval and the release of 10 000 particles takes 3 h. (2) The obtained particle distributions are combined with surface CO_2 fluxes at the location of each particle to calculate the contribution of the surface fluxes during this 7-day period to the observed concentration (ΔC). (3) The CO_2 concentration simulated by NIES TM at the location of each particle at the moment of coupling is averaged over the total number of particles to yield an initial CO_2 concentration for the Eulerian stage (C_{init}). This concentration includes the contribution by surface fluxes before the start of the Lagrangian stage. (4) The initial CO_2 concentration (C_{init}) and the concentration changes along the trajectories of the Lagrangian part (ΔC), as contributed by surface fluxes and transformations, are added together to give the predicted concentration at the observation time and location.

Consequently, the CO_2 concentration calculated by the coupled model, C_{cpld}, is expressed as

$$C_{\mathrm{cpld}} = \Delta C + C_{\mathrm{init}}. \quad (1)$$

GMDD
3, 2051–2070, 2010

ΔC can be calculated based on trajectory statistics (Seibert et al., 2004), and is expressed as

$$\Delta C = \frac{1}{M_o}\int_{T_b}^{T_e} dt \int dx \int dy \int dz\, m(\boldsymbol{r}) \frac{\delta C(\boldsymbol{r})}{\delta t}, \tag{2}$$

where M_o is the total mass of air particles released from the monitoring site; T_b and T_e are the beginning and end times of the back-plume trajectory calculations, respectively; and $m(\boldsymbol{r})$ is the particle density field, which can be expressed via individual particle positions as:

$$m(\boldsymbol{r}) = \sum_{i=1}^{N} \mu_i \cdot \delta(\boldsymbol{r} - \boldsymbol{r}_i), \tag{3}$$

where N is number of particles, $\mu_i = M_0/N$ is i-th particle mass, $\boldsymbol{r} = (x, y, z)$ is position vector, $\boldsymbol{r}_i$ is an i-th particle position and $\delta(\boldsymbol{r})$ is a Dirac delta function.

Assuming the surface flux is injected homogeneously into a near surface layer of thickness z_s, $\delta C/\delta t$, which is the rate of change of the near-surface CO_2 concentration contributed by a surface flux, can be approximated as

$$\frac{\delta C}{\delta t} = \frac{F(x, y, t)}{z_s}, \tag{4}$$

where F is the surface flux. We assume z_s = 300 m in this study and this height is approximately corresponding to the lowest model level of NIES TM. From Eqs. (2), (3) and (4), the following equation is derived:

$$\Delta C = \frac{1}{M_o}\int_{T_b}^{T_e} dt \int dx \int dy \int_{0}^{z_s} dz\, m(\boldsymbol{r}) \frac{F(x, y, t)}{z_s} \tag{5}$$

ΔC is calculated based on Eq. (5). In this study, a time interval dt of 1 h is assigned.

GMDD
3, 2051–2070, 2010

C_{init} is calculated as follows:

$$C_{\text{init}}(T_e) = \frac{1}{M_o}\int dx \int dy \int dz\, m(\boldsymbol{r}) C_{3\text{-D}}(x,y,z,T_e), \quad (6)$$

where $C_{3\text{-D}}$ is the CO_2 concentration in each simulation grid cell of NIES TM. Therefore, using Eq. (3) for particle concentration $m(\boldsymbol{r})$ both ΔC and $C_{\text{init}}(T_e)$ can be calculated without determining explicitly the global particle concentration field $m(\boldsymbol{r})$ in the Lagrangian part (FLEXPART), which is a convenient property when the flux F is given at very high resolution.

Forward calculations can also be performed using an LPDM (Eq. 5) alone, employing a crude representation of $C_{3\text{-D}}$, as tested by Stohl et al. (2009). However, to reproduce seasonal variations, at least 3 months of transport is required in our experience. Computing 10 000 particle plume transport for a 3-month period with FLEXPART for each 3-hourly observation is computationally expensive; therefore, it is not efficient to calculate seasonal variations in CO_2 using an LPDM alone. In contrast, the coupled model requires only a short period of back-plume trajectory calculations to reproduce seasonal variations.

Using the coupled model, we simulated variations in CO_2 concentrations at Barrow (USA), Samoa, American Samoa, and Hateruma (Japan). To calculate CO_2 concentrations, the coupled model is used to simulate the transport of the biospheric CO_2 tracer, the oceanic CO_2 tracer, and the anthropogenic CO_2 tracer. Biospheric CO_2 is simulated using CASA model fluxes (Randerson et al., 1997) and the ocean CO_2 tracer is based on air–sea fluxes reported by Takahashi et al. (2002). These monthly fluxes are converted into daily fluxes by linear interpolation. For the anthropogenic CO_2 tracer, we employ the flux of fossil fuel emissions produced by the Emissions Database for Global Atmospheric Research (EDGAR), version 4 (EDGAR, 2009). Fossil fuel emissions are kept constant throughout the simulation. All fluxes used in this study have a horizontal resolution of $1.0^\circ \times 1.0^\circ$.

FLEXPART is forced with analysis data of the Global Forecast System (GFS) model of NOAA/NCEP (National Centers for Environmental Prediction). NIES TM is driven by

GMDD
3, 2051–2070, 2010

reanalysis data of the NCEP/NCAR Reanalysis Project (Kalnay et al., 1996) and is run with a horizontal resolution of 2.5° × 2.5°, with 15 sigma levels.

To deseasonalize the CO_2 concentrations, we employ a running average method, as follows:

$$\tilde{C}_i = C_i - \frac{1}{n+1} \sum_{j=i-n/2}^{i+n/2} C_j, \quad (7)$$

where C_i is the CO_2 concentration corresponding to the sampling date–time (i), n is the time window for averaging (set to 90 days), and $\tilde{C}_i$ is the deseasonalized CO_2 concentration.

3 Results and discussion

Figure 1 shows the CO_2 concentrations calculated by NIES TM and the coupled model from January to March in 2003. The CO_2 concentrations are calculated year-round; however, to clearly show the difference between the two models, only 3 months of CO_2 variations are displayed in Fig. 1, in which the continuous observations are plotted together with the model results. Both the model results and observations are recorded at 3-h intervals, and the offset values are added to the original model outputs. The coupled model performs better than NIES TM in reproducing the observed sharp peaks – this is the main advantage of coupling an LPDM with a Eulerian grid model.

This advantage of the coupled model is especially pronounced in the case of Hateruma. During the winter season, air masses are transported from East Asia to Japan by the Asian monsoon. Consequently, the CO_2 concentration at Hateruma is strongly affected by emissions from East Asia. It is expected that the coupled model would be more useful for simulations at sites located in contaminated regions than for sites located in background regions.

As shown in Fig. 2, the coupled model performs better than the Eulerian model in simulating deseasonalized CO_2 concentrations, especially at Hateruma. Figure 3

GMDD
3, 2051–2070, 2010

shows the absolute value of the difference between deseasonalized model-predicted and observed CO_2 concentrations at Hateruma. As seen in Fig. 3, the coupled model yields the fewer difference with observation than NIES TM almost year-round, with visible reduction of the misfit during short-term high concentration events.

This is confirmed by the correlation coefficients and variance ratios between deseasonalized simulations and observations for the period 2002–2004 (Tables 1 and 2, respectively). The variance ratio is the standard deviation of the model-simulated concentrations normalized by the standard deviation of observed concentrations. The validation of model ability based on the correlation coefficients and variance ratios is the common method and employed by TransCom project (Patra et al., 2008). The values listed in Table 1 and 2 are calculated using year-round data, although the variance and correlations would become higher restricting to only the winter season in the case of Hateruma.

Table 1 lists the correlation coefficients between simulated and observed CO_2 concentrations. Data from the Barrow site show similar correlation coefficients between NIES TM and the coupled model. However, for Samoa and Hateruma, the coupled model shows better agreement with the observations. The difference in correlation coefficients between the coupled model and NIES TM exceeds 0.1 for each year. Figure 4 is the scatter plot which exhibits the relationship between model-predicted and observed CO_2 concentrations in synoptic scale for the period 2002–2004 at Hateruma. In Fig. 4, lines made by the linear least squares fitting technique are also displayed. As shown in the figure, almost all data appear to fit within plus or minus 4 ppm, with coupled model misfit being less than for NIES TM. The coupled model also shows the higher correlation coefficient than NIES TM as shown in Table 1.

Table 2 lists the variance ratios between simulated and observed CO_2 concentrations. The variance ratios calculated for the coupled model are closer to value “1” than those for NIES TM except Samoa. This indicates that coupling with LPDMs helps to compensate for smearing of the concentration fields that arises because of the numerical diffusion intrinsic to Eulerian models for the Barrow and Hateruma sites.

GMDD
3, 2051–2070, 2010

4 Conclusions

We developed a global coupled transport model comprising Lagrangian and Eulerian atmospheric transport models, and validated the coupled model by comparing simulation data with NIES and NOAA continuous observations. The coupled model performs well in reproducing both seasonal variations and synoptic-scale peaks in observational data. Unlike most other published implementations of coupled models, both of the model components in the present study (the Lagrangian part and the Eulerian part) are global. Therefore, the proposed model is readily applied to analyses of the global transport of long-lived tracers, which requires the resolving of both short and long time scales.

Medium-resolution Eulerian models can only resolve concentration variations at close to daily time scales. Thus, much useful information at shorter time scales is lost, including tracer correlations. In contrast, the coupled model can resolve concentration variations at an hourly time scale or less. Therefore, the coupled model performs better than a global Eulerian model alone in simulating synoptic-scale variability, and it can be used for analyses of variations in CO_2 due to synoptic-scale meteorological phenomena, without the need for nested regional-scale modeling.

The use of a coupled model enables calculations of surface flux contributions to tracer concentrations at a resolution higher than that of the meteorological data used in an LPDM, as in many cases the spatial scale of heterogeneity in surface fluxes is much smaller than the correlation radius of meteorological data. Accordingly, surface flux data with very high resolution (e.g., several kilometers) can be used for forward transport modeling without compromising the effective resolution of tracer transport.

Acknowledgements. Authors are grateful to Andreas Stohl for providing the FLEXPART model code. This work was supported by the Global Environmental Research Fund of the Ministry of Environment, Japan.

GMDD
3, 2051–2070, 2010

References

EDGAR: European Commission, Joint Research Centre (JRC)/Netherlands Environmental Assessment Agency (PBL) Emission Database for Global Atmospheric Research (EDGAR), release version 4.0., available at: http://edgar.jrc.ec.europa.eu, 2009.

Gloor, M., Bakwin, P., Hurst, D., Lock, L., Draxler, R., and Tans, P.: What is the concentration footprint of a tall tower?, J. Geophys. Res., 106, D16, 17831–17840, doi:10.1029/2001JD900021, 2001.

Godunov, S. K.: A difference scheme for numerical solution of discontinuous solution of hydrodynamic equations, Math. Sbornik, 47, 271–306, 1959 (in Russian, translated by the US Joint Publ. Res. Service, JPRS 7226, 1969).

Gurney, K. G., Mendoza, D. L., Zhou, Y., Fischer, M. L., Miller, C. C., Geethakumar, S., and de la Rue du Can, S.: High resolution fossil fuel combustion CO_2 emission fluxes for the United States, Environ. Sci. Technol., 43, 5535–5541, doi:10.1021/es900806c, 2009.

Kalnay, E., Kanamitsu, M., Kistler, R., Collins, W., Deaven, D., Gandin, L., Iredell, M., Saha, S., White, G., Woollen, J., Zhu, Y., Chelliah, M., Ebisuzaki, W., Higgins, W., Janowiak, J., Mo, K. C., Ropelewski, C., Wang, J., Leetmaa, A., Reynolds, R., Jenne, R., and Joseph, D.: The NCEP/NCAR 40-Year Reanalysis Project, Bull. Am. Meteorol. Soc., 70, 437–471, 1996.

Kannari, A., Tonooka, Y., Baba, T., and Murano, K.: Development of multiple-species 1×1 km resolution hourly basis emissions inventory for Japan, Atmos. Environ., 41, 3428–3439, doi:10.1016/j.atmosenv.2006.12.015, 2007.

Lin, J. C., Gerbig, C., Wofsy, S. C., Andrews, A. E., Daube, B. C., Davis, K. J., and Grainger, C. A.: A near-field tool for simulating the upstream influence of atmospheric observations: The Stochastic Time-Inverted Lagrangian Transport (STILT) model, J. Geophys. Res., 108, 4493, doi:10.1029/2002JD003161, 2003.

Lin, J. C., Gerbig, C., Wofsy, S. C., Chow, V. Y., Gottlieb, E., Daube, B. C., and Matross, D. M.: Designing Lagrangian experiments to measure regional-scale trace gas fluxes, J. Geophys. Res., 112, D13312, doi:10.1029/2006JD008077, 2007.

Lin, J. C., Gerbig, C., Wofsy, S. C., Daube, B. C., Matross, D. M., Chow, V. Y., Gottlieb, E., Andrews, A. E., Pathmathevan, M., and Munger, J. W.: What have we learned from intensive atmospheric sampling field programmes of CO_2?, Tellus B, 58, 331–343, doi:10.1111/j.1600-0889.2006.00202.x, 2006.

Maksyutov, S., Patra, P. K., Onishi, R., Saeki, T., and Nakazawa, T.: NIES/FRCGC global

GMDD
3, 2051–2070, 2010

atmospheric tracer transport model: description, validation, and surface sources and sinks inversion, Journal of the Earth Simulator, 9, 3–18, 2008.

Mukai, H., Katsumoto, M., Ide, R., Machida, T., Fujinuma,Y., Nojiri, Y., Inagaki, M., Oda, N., and Watai, T.: Characterization of atmospheric CO_2 observed at two-background air monitoring stations (Hateruma and Ochi-ishi) in Japan, 6th International Carbon Dioxide Conference, Sendai, Japan, 1–5 October 2001, Extended Abstract, Vol. 1 AT16, 108–111, 2001.

Oda, T. and Maksyutov, S.: A very high-resolution global fossil fuel CO_2 emission inventory derived using a point source database and satellite observations of nighttime lights, 1980–2007, Atmos. Chem. Phys. Discuss., 10, 16307–16344, doi:10.5194/acpd-10-16307-2010, 2010.

Olivier, J. G. J., Pulles, T., and van Aardenne, J. A.: Part III: Greenhouse gas emissions: 1. Shares and trends in greenhouse gas emissions; 2. Sources and Methods; 3. Total greenhouse gas emissions, in: CO_2 Emissions from Fuel Combustion 1971–2006, 2008 Edition, International Energy Agency (IEA), Paris, III.1-III.47, 2008.

Paris, J.-D., Stohl, A., Ciais, P., Nédélec, P., Belan, B. D., Arshinov, M. Yu., and Ramonet, M.: Source-receptor relationships for airborne measurements of CO_2, CO and O_3 above Siberia: a cluster-based approach, Atmos. Chem. Phys., 10, 1671–1687, doi:10.5194/acp-10-1671-2010, 2010.

Patra, P. K., Law, R. M., Peters, W., Rödenbeck, C., Takigawa, M., Aulagnier, C., Baker, I., Bergmann, D. J., Bousquet, P., Brandt, J., Bruhwiler, L., Cameron-Smith, P. J., Christensen, J. H., Delage, F., Denning, A. S., Fan, S., Geels, C., Houweling, S., Imasu, R., Karstens, U., Kawa, S. R., Kleist, J., Krol, M. C., Lin, S.-J., Lokupitiya, R., Maki, T., Maksyutov, S., Niwa, Y., Onishi, R., Parazoo, N., Pieterse, G., River, L., Satoh, M., Serrar, S., Taguchi, S., Vautard, R., Vermeulen, A. T., and Zhu, Z.: TransCom model simulations of hourly atmospheric CO_2: Analysis of synoptic-scale variations for the period 2002–2003, Global Biogeochem. Cy., 22, GB4013, doi:10.1029/2007GB003081, 2008.

Randerson, J. T., Thompson, M. V., Conway, T. J., Fung, I. Y., and Field, C. B.: The contribution of terrestrial sources and sinks to trends in the seasonal cycle of atmospheric carbon dioxide, Global Biogeochem. Cy., 11, 535–560, doi:10.1029/97GB02268, 1997.

Rodean, H. C.: Stochastic Lagrangian models of turbulent diffusion, Meteorological Monograph Series, 26(48), American Meteorological Society, Boston, 1996.

Seibert, P. and Frank, A.: Source-receptor matrix calculation with a Lagrangian particle dispersion model in backward mode, Atmos. Chem. Phys., 4, 51–63, doi:10.5194/acp-4-51-2004,

GMDD

3, 2051–2070, 2010

2004.
Stohl, A., Hittenbeger, M., and Wotawa, G.: Validation of the Lagrangian particle dispersion model FLEXPART against large scale tracer experiments, Atmos. Environ., 32, 4245–4264, doi:10.1016/S1352-2310(98)00184-8, 1998.
Stohl, A., Kim, J., Li, S., O'Doherty, S., Mhle, J., Salameh, P. K., Saito, T., Vollmer, M. K., Wan, D., Weiss, R. F., Yao, B., Yokouchi, Y., and Zhou, L. X.: Hydrochlorofluorocarbon and hydrofluorocarbon emissions in East Asia determined by inverse modeling, Atmos. Chem. Phys., 10, 3545–3560, doi:10.5194/acp-10-3545-2010, 2010.
Stohl, A., Seibert, P., Arduini, J., Eckhardt, S., Fraser, P., Greally, B. R., Lunder, C., Maione, M., Mühle, J., O'Doherty, S., Prinn, R. G., Reimann, S., Saito, T., Schmidbauer, N., Simmonds, P. G., Vollmer, M. K., Weiss, R. F., and Yokouchi, Y.: An analytical inversion method for determining regional and global emissions of greenhouse gases: Sensitivity studies and application to halocarbons, Atmos. Chem. Phys., 9, 1597–1620, doi:10.5194/acp-9-1597-2009, 2009.
Takahashi, T., Sutherland, S. C., Sweeney, C., Poisson, A., Metzl, N., Tilbrook, B., Bates, N., Wanninkhof, R., Feely, R. A., Sabine, C., Olafsson, J., and Nojiri, Y.: Global sea-air CO_2 flux based on climatological surface ocean pCO_2, and seasonal biological and temperature effects, Deep-Sea Res. Pt. II, 49, 1601–1622, doi:10.1016/S0967-0645(02)00003-6, 2002.
Thompson, R.: Numeric calculation of turbulent diffusion, Q. J. Roy. Meteor. Soc., 97, 93–98, doi:10.1002/qj.49709741109, 1971.
Thoning, K. W., Kitzis, D. R., and Crotwell, A.: Atmospheric carbon dioxide dry air mole fractions from quasi-continuous measurements at Barrow, Alaska; Mauna Loa, Hawaii; American Samoa; and South Pole, 1973-2006, Version: 2009-04-10, Path: ftp://ftp.cmdl.noaa.gov/ccg/co2/in-situ/, 2007.
Trusilova, K., Rödenbeck, C., Gerbig, C., and Heimann, M.: Technical Note: A new coupled system for global-to-regional downscaling of CO_2 concentration estimation, Atmos. Chem. Phys., 10, 3205–3213, doi:10.5194/acp-10-3205-2010, 2010.
Uliasz, M.: Lagrangian particle dispersion modeling in mesoscale applications, in: Environmental Modeling Vol. II, edited by: Zannetti, P., Computational Mechanics Publications, Southampton, 71–101, 1994.
Vermeulen, A. T., Pieterse, G., Hensen, A., van den Bulk, W. C. M., and Erisman, J. W.: COMET: a Lagrangian transport model for greenhouse gas emission estimation – forward model technique and performance for methane, Atmos. Chem. Phys. Discuss., 6, 8727–

GMDD
3, 2051–2070, 2010

8779, 2006,
http://www.atmos-chem-phys-discuss.net/6/8727/2006/.
Warneke, C., Bahreini, R., Brioude, J., Brock, C. A., de Gouw, J. A., Fahey, D. W., Froyd, K. D., Holloway, J. S., Middlebrook, A., Miller, L., Montzka, S., Murphy, D. M., Peischl, J., Ryerson, T. B., Schwarz, J. P., Spackman, J. R., and Veres, P.: Biomass burning in Siberia and Kazakhstan as an important source for haze over the Alaskan Arctic in April 2008, Geophys. Res. Lett., 36, L02813, doi:10.1029/2008GL036194, 2009.
Wilson, J. D. and Sawford, B. L.: Review of Lagrangian stochastic models for trajectories in the turbulent atmosphere, Bound.-Lay. Meteorol., 78, 191–210, doi:10.1007/BF00122492, 1996.
Zannetti, P.: Particle modeling and its application for simulating air pollution phenomena, in: Environmental Modeling, edited by: Meli, P., Computational Mechanics Publications, Southampton, 211–241, 1992.

GMDD
3, 2051–2070, 2010

Table 1. Correlation coefficients between simulated and observed deseasonalized CO_2 values.

Site code	Year	NIES TM	Coupled model
BRW	2002	0.55	0.45
	2003	0.59	0.59
	2004	0.64	0.61
SMO	2002	0.48	0.60
	2003	0.47	0.67
	2004	0.57	0.69
HAT	2002	0.45	0.55
	2003	0.49	0.62
	2004	0.43	0.56

GMDD
3, 2051–2070, 2010

Table 2. Variance ratios between simulated and observed deseasonalized CO_2 values.

Site code	Year	NIES TM	Coupled model
BRW	2002	0.77	1.03
	2003	0.94	1.00
	2004	0.66	0.81
SMO	2002	1.58	1.66
	2003	1.61	1.68
	2004	1.76	2.10
HAT	2002	1.07	1.11
	2003	1.33	1.07
	2004	1.29	1.11

GMDD
3, 2051–2070, 2010

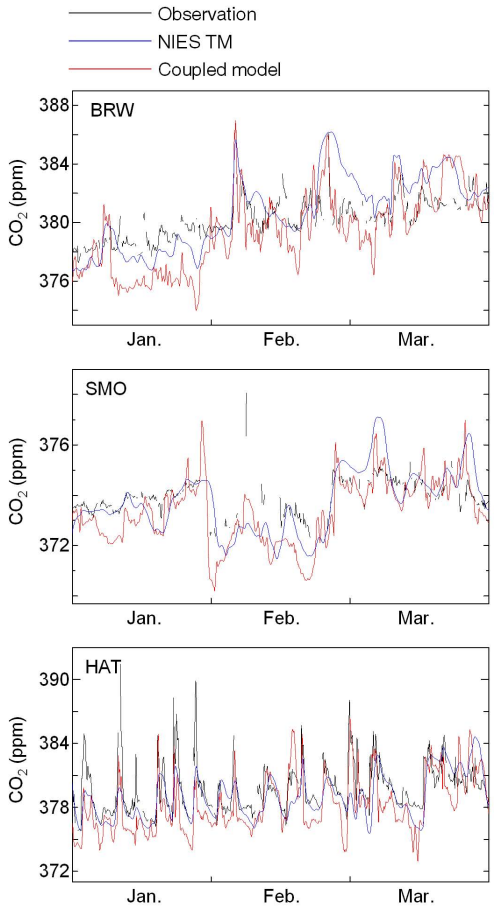

Fig. 1. CO_2 concentrations at Barrow (BRW, top), Samoa (SMO, middle), and Hateruma (HAT, bottom) from January to March 2003. Black lines: observations; blue lines: NIES TM; red lines: coupled model.

GMDD
3, 2051–2070, 2010

Simulation of atmospheric carbon-dioxide variability

Y. Koyama et al.

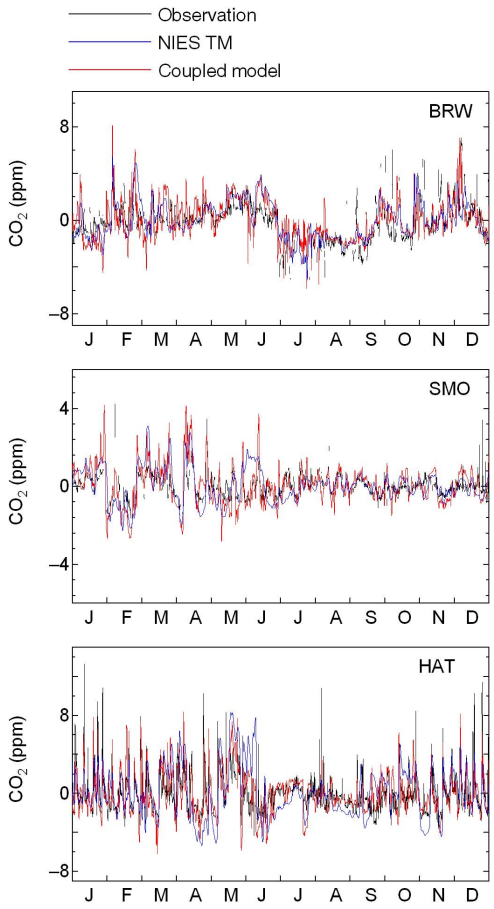

Fig. 2. Deseasonalized CO_2 concentrations at Barrow (BRW, top), Samoa (SMO, middle), and Hateruma (HAT, bottom) for 2003. Black lines: observations; blue lines: NIES TM; red lines: coupled model.

GMDD
3, 2051–2070, 2010

Simulation of atmospheric carbon-dioxide variability

Y. Koyama et al.

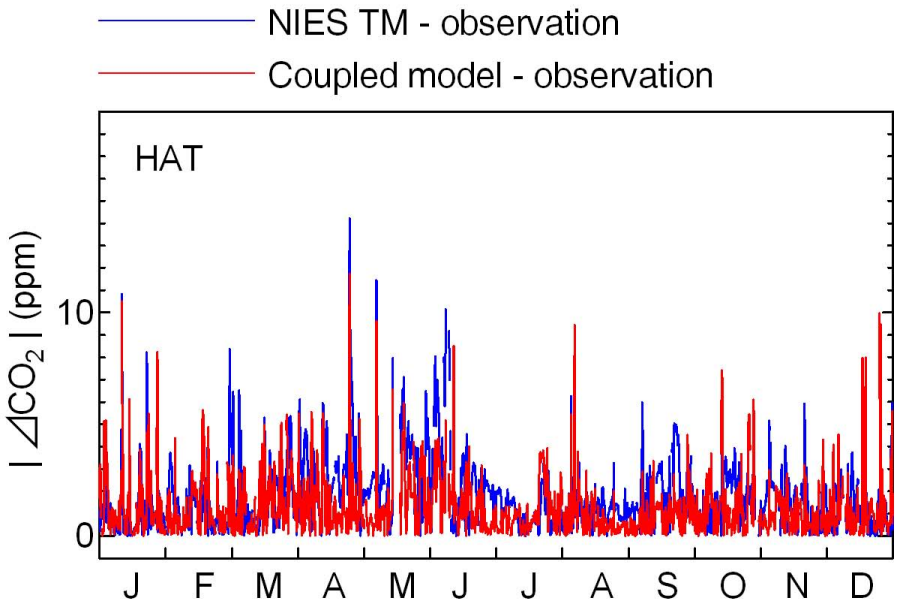

Fig. 3. Absolute value of the difference between deseasonalized model-predicted and observed CO_2 concentrations at Hateruma. Blue lines: NIES TM-observations; red lines: coupled model-observations.

GMDD
3, 2051–2070, 2010

Simulation of atmospheric carbon-dioxide variability

Y. Koyama et al.

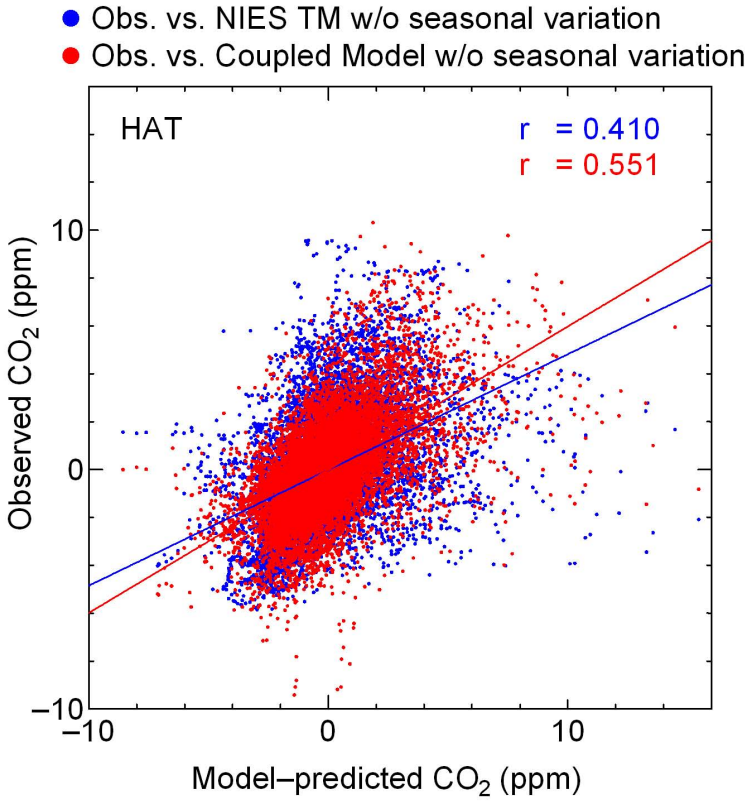

Fig. 4. Scatter plot which exhibits the relationship between model-predicted and observed CO_2 concentrations in synoptic scale for the period 2002–2004 at Hateruma. Blue circle: NIES TM-observation; red circle: coupled model-observation.

GMDD
3, 2051–2070, 2010

Simulation of atmospheric carbon-dioxide variability

Y. Koyama et al.